Numerical Simulations and Experimental Studies on the Formability of Drawing Quality Steel in Single Point Incremental Forming

Zeradam Yeshiwas, A. Krishniah*
Department of Mechanical Engineering, College of Engineering, Osmania University, Hyderabad, India
**zeruhulu@gmail.com*

ABSTRACT

Based on numerical simulation and experimental studies the process parameter optimization on the formability using a 1 mm thickness Drawing Quality Steel(CR2) in Single Point Incremental Forming (SPIF)was studied. The sample shape chosen was the hayperbolic cone and fabricated using different parameter leveles. A model of numeric simulation was developed in ABAQUS explicit and then experimentally verified using a CNC milling machine. The influence of three significant control factors, namely tool radius, feeding rate, and step depth on the formability was studied. Optimization of process parameters was conducted using the L9 Taguchi orthogonal array. For optimal formability, to assess the optimum combination of process parameters, a signal noise (S/N) ratio was used. The percentage contribution of the method parameters to formability was determined by the Study of Variance (ANOVA). The findings of the study indicated that the depth of the step followed by feed rate and tool radius, was the dominant factor influencing formability. Furthermore, a good agreement (<8% error) between the numerical simulation and experimental study was seen. The study based on the Taguchi configuration of the study shows that at a feed rate (A2) 1000 mm/min, with tool radius (B1) 8 mm, and with step depth (C2) 0.8 mm, the optimal conditions for maximum formability were achieved.

Keywords: *Drawing Quality Steel, Formability, Incremental forming, Numerical simulation, Thickness distribution*

ISSN 1823-5514, eISSN2550-164X
Received for review: 2020-09-11
Accepted for publication: 2020-12-21
Published: 2021-01-15

Nomenclature

ϵ_T: True strain	αp: Maximum Forming angle
Δt: Time increment	Δd: Error
ΔZ: Step depth	d_e: Depth at fracture
α_e: Wall angle at fracture	DF: Degrees of freedom
ds: Depth at minimum thinning	F: Variance
α_s: Wall angle at maximum thinning	MS: Mean square
C_d: Dilatational wave speed	P: Test static
Le: Element length	SS: Sum of squares

Introduction

Formability in SPIF can be measured using one of the three different methods, i.e. measuring the maximum wall-angle, taking into account the maximum formability depth achieved, or examining the maximum reduction in thickness achieved without failure. Various studies have assessed the impact of process parameters on SPIF formability, i.e., step depth, the radius of the forming tool, and feed rate. This section has attempted to summarize the literature concerning the impact of process parameters in SPIF.

Many scholars have found the impact of step depth on formability and some of the researchers concluded that the higher value of the Step-depth increases formability [1]-[5]. Another group of researchers [6]-[8] labeled the effect of step depth on formability and reported that the lower step depth value improves formability.

There have been several reports on the impact of the forming-tool radius on formability. Recent work covers [4], [5], [9]-[11], and the researchers concluded that formability increases when the radius of the tool increases. Several authors including [7], [8], [12]-[14] have used experimental studies to test the impact of tool radius on formability. The researchers concluded that formability increases as the radius of the forming tool decreases. For another study, Malwad [13] explored the effect on the formability of the tool radius. In the study, 3 mm and 6 mm radius tools were used for performing the fabrication. The work has been an experimental inquiry into an aluminum alloy. The study concluded that formability improves to some degree, as tool radius decreases.

A considerable amount of research on the effect of feed rate on formability has been published including [5], [7], [12], [14] and found that the formability increases as the feed rate decreases. Bagudanch [4] also assessed the impact of feed rate on formability in SPIF. The study was carried out using the experimental process, and the material being tested was a polymer. The researchers conclude with a high feed rate, that formability increases. Besides, Golabi [9] and Uheida [15] assessed the impact of feed

rate on formability in SPIF. These experiments were carried out using numerical simulation and experimental methods, and the research materials included steel and titanium. The researchers conclude that there is no significant effect of feed rate on formability.

Hussain [22] and Al-Ghamdi [23] suggested that the tool diameter could be optimized to achieve the maximum improvement in formability. Obikawa [24], Hussain [25] and Davarpanah [2] are some of the researchers who conclude that step depth should be optimized to achieve the greatest improvement in formability. Ambrogio [26], suggested that the feed rate should be optimized to achieve the maximum improvement in formability.

It was observed that much of the previous research in formability studies focused on aluminium alloys and had less concern for other material classes. Therefore in this study, cold-rolled drawing grade steel material was used. Furthermore, the literature review reveals contradictory findings about the effect on the formability of tool diameter, feed rate, and step depth. Therefore process parameter optimization was achieved in this study using Taguchi experimental design.

Material and Methods

This study aimed to investigate the effect of process parameters on the formability and optimization of process parameters using drawing quality (CR2) steel sheets in single point incremental forming (SPIF), which is one of the widely used materials in the automotive industry. Tables 1 and Table 2 respectively describe the composition and mechanical properties of the CR2 steel sheet.

Table 1: Composition of drawing quality steel

Quality		Constituent, Percent, *Max*			
Designation	Name	Carbon	Manganese	Sulfur	Phosphorus
CR2	Drawing	0.12	0.50	0.035	0.040

Table 2: Mechanical properties of drawing quality steel

Quality	Yield Stress *R*e, MPa	Tensile Strength *R*m, MPa	Elongation Percent, *A*, *Min*
Designation			*L*o = 80 mm
CR2	240 *Max*	370 *Max*	30

To obtain the true stress-strain curve of Drawing Quality (CR2) steel, the uniaxial Tension test was conducted with a sheet thickness of 1 mm. The specifications of the specimens are obtained according to the ISO 6892-1:2009 standard. Stress and strain are computed from measurements in a tension test of the tensile force, F, and the elongation, ΔL (load-displacement data). The true stress-strain data from the tensile test is approximated using power low as given in Equation (1).

$$\sigma_T = 568\varepsilon_T^{\,0.23} \tag{1}$$

Figure 1 depicted the procedure that was used for the experimental and numerical studies.

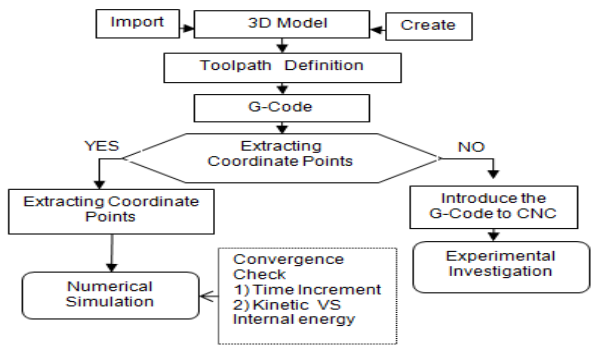

Figure 1: Method for the FEM simulation and experimental study.

A hyperbolic-cone component with a top opening diameter of 140 mm and a wall angle varying from 32 ° to 85 ° (Figure 2) was the sample shape chosen for the conduct of numerical simulation and experimental investigation.

The two most common methods to define the tool path in SPIF [20] are the contour and the spiral toolpath strategies. In this analysis, using CAM software, the contour toolpath was developed and the coordinate points were extracted using the Microsoft Excel formula [16], [17]. The coordinate points were then introduced to define displacement in the numerical simulation, whereas the G-code was directly introduced to the three-axis CNC Mill for the fabrication of the sample parts. Forming time was estimated using the relationship between feed rate and the total forming distance.

Taguchi Design of experiment and NOVA analysis has been done using MINITAB 19 software. The model of the finite element was validated by finding the maximum depth at minimum thinning and comparing with the

depth at the crack with the physical experiment. Error assessment was then made between the finite element model and the physical experiment.

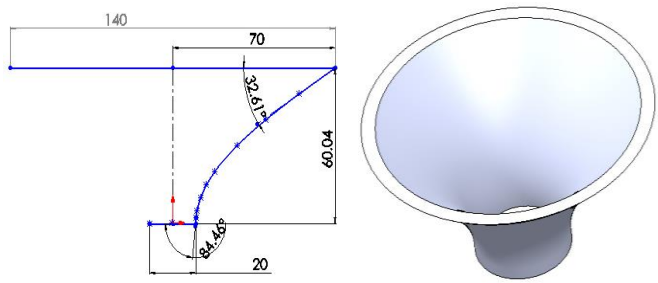

a) b)

Figure 2: Hyperbolic-cone chosen as a sample shape to study the formability a) two-dimensional view, and b) three-dimensional view.

Finite Element Model

In ABAQUS software, the finite element model was developed. The explicit approach of ABAQUS was selected to minimise the long computational time. The blank is modelled as a square measuring 290 mm X 290 mm X 1 mm and fixed at the four edges of the square (Figure 3). Blank is defined as a deformable body and meshed with shell elements (S4R). For mesh generation the approximate element size was 2 mm. A friction coefficient of 0.15 was applied between tool and forming surface. Hemisphere forming tools with a radius of 4 mm, 5 mm, and 6 mm have been chosen and defined as rigid analytical parts. The material properties introduced and position vs time data was defined as the displacement of the tool.

Mass scaling was introduced to reduce the time needed for simulations. A convergence check was done to find a bounded solution. Convergence check was done using two approaches firstly by checking the time increment, i.e., a convergent solution is obtained if the time increment (Δt) is less than the stable time increment (Δt_{min}). The stability limit is the ratio between the characteristic length of the element and the wave speed.

$$\Delta t = \frac{L_e}{Cd} \tag{2}$$

where element length, Le, and the dilatational wave speed of the material, Cd.

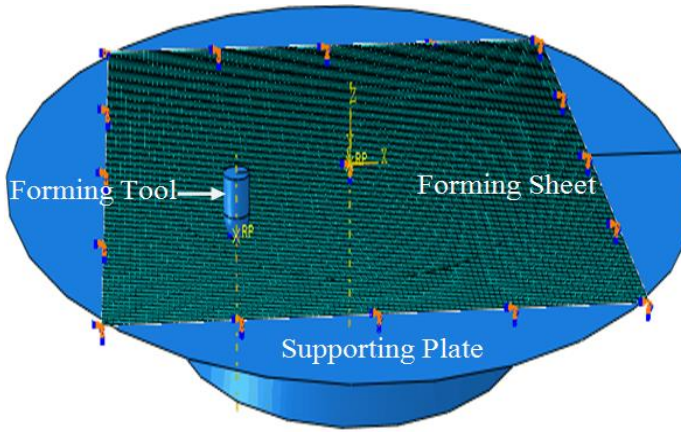

Figure 3: Single point incremental forming model.

The second approach is by checking the ratio of kinetic energy to internal energy. The ratio of kinetic energy to internal energy does not get too large, typically less than 10% [17, 21]. Figure 4 shows the kinetic energy to internal energy ratio in forming the hyperbolic-cone. Both time increment and the ratio of internal energy to kinetic energy have been satisfied in all numerical simulations.

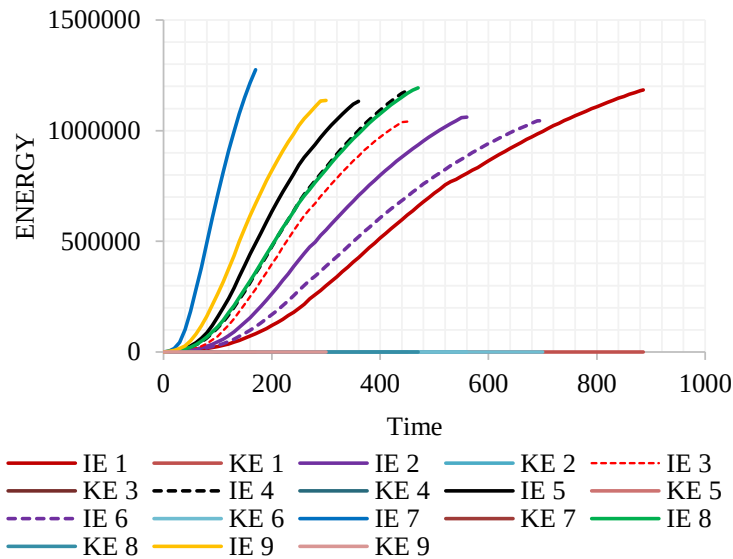

Figure 4: Internal energy combined with kinetic energy history.

Experimental setup

For the forming process, hemispheric tipped forming tools of a different radius of 4mm, 5 mm, and 6 mm were selected as shown in Figure 5. The forming tool moved along the path created from the CAM package until a crack was observed. The fixture for the work holding was mounted on a machine table with three axes CNC Mill, as shown in Figure 6. The material used in the present study was Cold rolled steel sheet (CR2/Drawing quality) 290 mm*290 mm*1 mm in dimension. In the forming process, drawing quality sheets of metal were fastened along their edges in a specially built fixture that was placed on the CNC machine table. Oil was applied to minimize friction between the forming tool and the blank surface.

Figure 5: Forming tools with Φ8, Φ10 and Φ12 diameter spherical end.

Figure 6: Experimental setup for single point incremental forming.

Taguchi Design of Experiment

The study aims to find the formability of drawing quality steel sheets (CR2) in the SPIF process through numerical simulations and experiments. The study also aims to find the optimum combination of factors that influence the formability. Several factors affect formability. However, in this study, the tool diameter, feed rate, and step depth were considered as most prominent once and included as an input factor.

As the number of factors is 3 with each at three levels, the standard orthogonal array L9 (33) was selected (Table 3) for the study using the array selection table [19]. Therefore, nine experiments to be conducted with factor combination as stipulated in the L9 (33) array, as indicated in Table 4.

Table 3: Factors and levels chosen for experimental design

			Factor Levels		
Factors	Symbol	Units	1	2	3
Feed	A	mm/min	800	1000	1500
Tool diameter	B	mm	8	10	12
Step	C	mm	0.5	0.8	1

Table 4: Experimental layout L9 (33) orthogonal array

Experiment No.	A	B	C
1	800	8	0.5
2	800	10	0.8
3	800	12	1
4	1000	8	0.8
5	1000	10	1
6	1000	12	0.5
7	1500	8	1
8	1500	10	0.5
9	1500	12	0.8

The highest value of formability angle or forming depth is significant for formability improvement. For this reason, the ‘‘larger-the-better’’ equation was used for the calculation of the S/N ratio. For this objective S/N ratio is defined by Equation 3 according to the Taguchi method.

$$S/N = -10\log\left[\frac{1}{n}\sum_{1}^{n} y_i^{\,2}\right] \tag{3}$$

Result and discussion

Numerical Simulation Result

Based on the Taguchi designs of the experiment, hyperbolic-cone samples were formed. Following the successful execution of the numerical simulation for the sample part, the post-processing was done to find the maximum depth at a minimum thinning. For all combinations of factors, the shell thickness contour plot for the formed parts is plotted as shown in Figure 7.

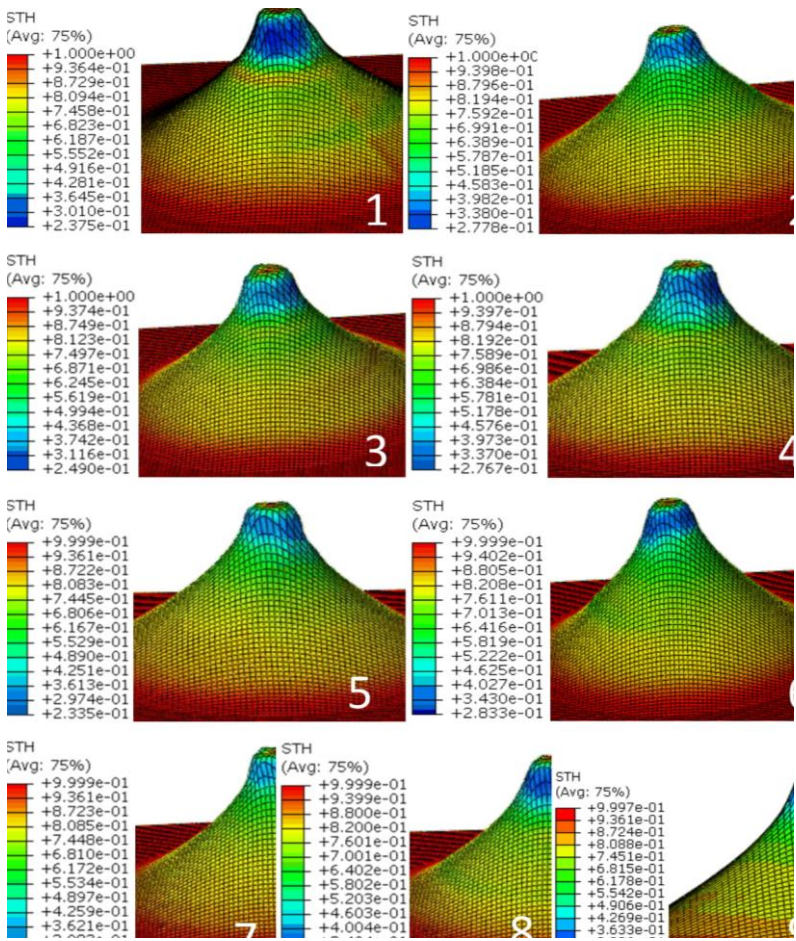

Figure 7: Thickness distribution contour plot under the condition of different combinations of process parameters for trial 1 to 9.

Using the contour of the SHT (Shell thickness) and the path option, the distance "Z" along the path (depth) was found at the maximum thinning. Figure 8 shows the depth measurement method. The measurement starts from the undeformed area, and ends with the maximum thinning at the nodal level. To validate the proposed FE model; the simulated forming depth was executed from the contour plot as shown in Figure 9, Figure 10 and Figure 11, and compared with experimental data.

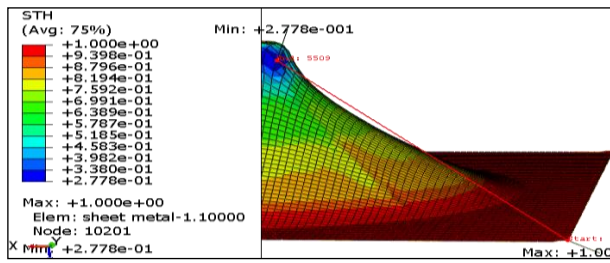

Figure 8: Depth measurement method at a maximum thinning.

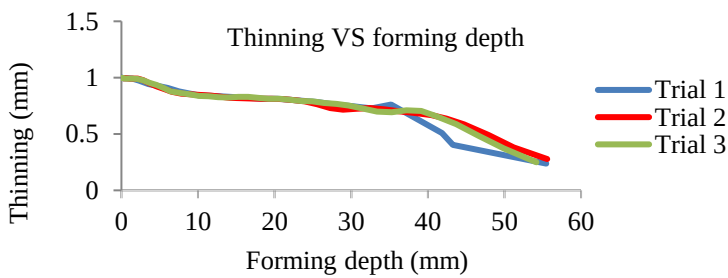

Figure 9: Distribution of thickness with depth for trial 1 trial 2 and trial 3.

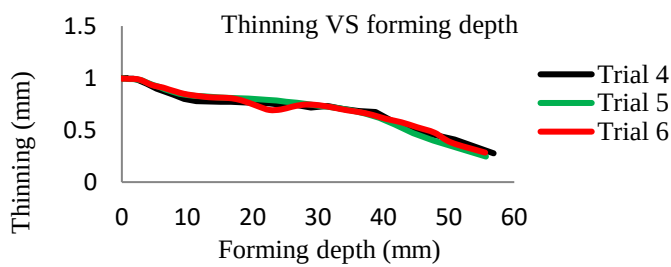

Figure 10: Distribution of thickness with depth for trial 4 trial 5 and trial 6.

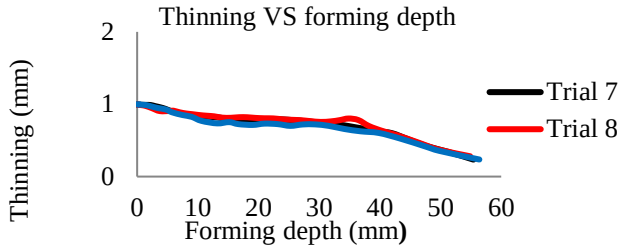

Figure 11: Distribution of thickness with depth for trial 7 trial 8 and trial 9.

Experimental Result

As shown in Figure 12, fabrication was performed for all the experimental combinations according to Taguchi L9 (3^3) orthogonal array to confirm the formablity predicted in the numerical simulation. The fabrication was stopped when the crack is begun. After the fabrication of the sample parts, the component depth up to the fracture was measured using Vernier Height Gauge as shown in Figure 13.

Figure 12: Parts formed based of L9 (3^3) design of experiment.

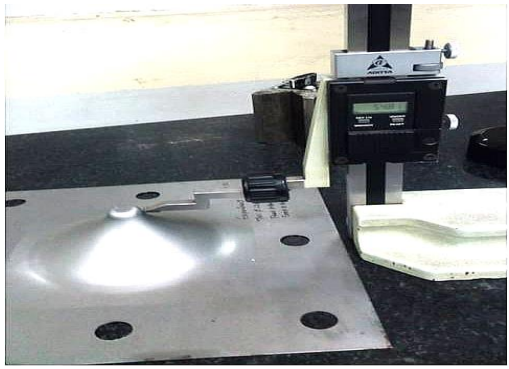

Figure 13: Depth measurement method using Vernier Height Gauge.

Figure 14 shows the Parabolic-cone with an initial opening radius of 70 mm was formed on the CNC milling machine until the crack is formed to measure the depth at the crack.

Figure 14: Magnified view of the crack formed in experiment 1.

In SPIF, One of the widely used ways of finding the maximum formability at which the material can be formed before failure occurs is the maximum wall angle (φmax) [1, 5]. The forming sheet material failure occurs during the SPIF process, as the forming depth of the parts increases. Forming depth can therefore be used as a formality measure [9, 11]. In this paper, Both the maximum angle of the wall at a crack and the maximum forming depth achieved at failure or maximum thinning were used to evaluate the formability.

The angle corresponding to the depth at a crack is called the maximum formability angle and computed using Equation 4 [7, 18].

$$\alpha_p = \tan^{-1}\left(\frac{\Delta Z}{\Delta X}\right) \tag{4}$$

In the above equation, ΔZ/ΔX gives the slope at any point p on the toolpath and represents the wall angle at p. Table 5 describes the findings obtained from the measurement of the maximum forming angle and depth at the crack.

Error Evaluation

When the fracture occurs in the experimental trials, the depth at fracture (de) were measured and compared with the depth at minimum thinning (ds) achieved from the numerical simulation. Figure 12 shows the fabricated parts after experiments, and the corresponding simulations depicted in Figure 7. To verify the accuracy of the proposed prediction of formability, the relative error between the simulation and physical experiment forming depth was calculated as shown in Table 5 using Equation (5).

$$\Delta d(\%) = \frac{|d_e - d_s|}{d_e} * 100\% \tag{5}$$

$$\Delta \alpha(\%) = \frac{|\alpha_e - \alpha_s|}{\alpha_e} * 100\% \tag{6}$$

Table 5: Formability depth, maximum formability angle and error

Trial No.	Simulation ds (mm)	Fabricated de (mm)	Error Δd (%)	Simulation α_s(°)	Fabricated α_e(°)	Error Δα%
1	55.45	53.79	3.09	79.11	75.74	4.45
2	55.58	54.17	2.61	79.69	76.5	4.17
3	54.68	53.93	1.39	76.93	75.93	1.32
4	56.84	55.65	2.13	82.733	79.89	3.56
5	55.67	54.55	2.05	79.38	77.81	2.02
6	55.55	53.99	2.88	78.58	75.96	3.45
7	55.42	53.79	3.03	79.41	75.74	4.85
8	53.13	52.44	1.32	73.07	72.77	0.41
9	56.39	54.81	2.89	81.94	77.6	5.59

αe, wall angle at fracture; αs, wall angle at maximum thinning

Optimum combination of process parameters

Depth at the crack and maximum formability angle were measured via the experimental design for each combination of the control factors by using Taguchi techniques, optimization of the measured control factors were provided by signal-to-noise (S/N) ratios. Table 6 shows the values of the S/N ratios for observations of depth at the crack and at the minimum thinning.

Table 6: the experiment response for the formability

Experimental Results		Numerical Simulation	
1/(S^2)	S/N	1/(S^2)	S/N
0.000346	34.61	0.000325	34.88
0.000341	34.68	0.000324	34.9
0.000344	34.64	0.000334	34.76
0.000323	34.91	0.00031	35.09
0.000336	34.74	0.000323	34.91
0.000343	34.65	0.000324	34.89
0.000346	34.61	0.000326	34.87
0.000364	34.39	0.000354	34.51
0.000333	34.78	0.000314	35.03

The level values of control factors for the maximum forming depth or forming angle given in Table 7 and 8 are shown in graph forms in Figures 15(a) and Figure 15(b). Optimal forming parameters of the control factors for maximizing the forming depth can be easily determined from these graphs. The best level for each control factor was found according to the highest S/N ratio in the levels of that control factor.

Table 7: shows the optimal levels of control factors (fabricated)

	Mean S/N ratio(dB)			
Parameter	Level 1	Level 2	Level 3	Max-min
Feed Rate	34.64	34.76	34.59	0.17
Tool Radius	34.71	34.60	34.68	0.11
Step Depth	34.55	34.78	34.66	0.23

Table 8: shows the optimal levels of control factors (simulation)

Parameter	Mean S/N ratio(dB			
	Level 1	Level 2	Level 3	Max-min
Feed Rate	34.84	34.97	34.80	0.17
Tool Radius	34.95	34.77	34.89	0.18
Step Depth	34.76	35.01	34.85	0.25

In the numerical simulation, the levels and S/N ratios for the factors giving the best formability depth and angle value were specified as factor A (Level 2, S/N = 34.97), factor B (Level 1, S/N = 34.95), and factor C (Level 2, S/N = 35.01). In the experimental study, the levels and S/N ratios for the factors giving the best formability depth and angle value were specified as factor A (Level 2, S/N = 34.76), factor B (Level 1, S/N = 34.71), and factor C (Level 2, S/N = 34.78). In other words, optimum formability was obtained at a feed rate (A2) 1000 mm/min, with tool radius (B1) 8 mm and with step depth (C2) 0.8 mm (Figure 15(b)). From this, it can be concluded that the best setting factor to achieve maximum formability is A2B1C2.

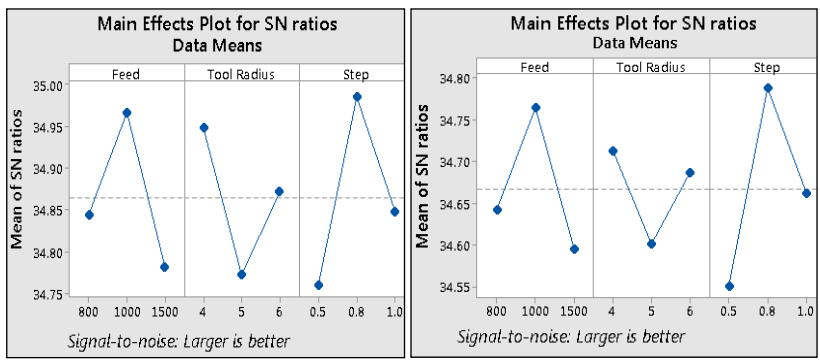

(a) (b)

Figure 15: Optimum combinations of factors for the maximum forming depth (a) Numerical Simulation and (b)Fabricated part.

Confirmation experiment

After the optimal levels of forming parameters are identified, a confirmation test is necessary to check the accuracy of the analysis. However, the optimal setting of process parameters is found among the experiments. The confirmation experiment presents the maximum value of depth at the crack in experiment 4 with a combination setting of A2B1C2. The maximum wall angle achieved is 79.89°, and the depth at a crack is 55.65. This value is higher than the value achieved for all combinations of parameters during experimentation.

In the numerical simulation, the confirmation experiment presents the maximum value of depth at the minimum thinning is achieved in experiment 4 with a combination setting of A2B1C2. The maximum wall angle achieved is 82.73°, and the depth at a crack is 56.84. This value is higher than the value achieved for all combinations of parameters during simulation.

Kurra [7] reported the same results, using Extra Deep Drawing (EDD) steel in the SPIF process to investigate the impact of process parameters on maximum wall angle. The optimum process parameters for maximum formality to be tool diameter at level 1 (6 mm) and step depth at level 2 (1.1 mm). Gulti [12] and Oleksik [8] also stated that the formability is increased by decreasing the tool diameter.

Analysis of variance (ANOVA)

Table 9 and Figure 10 show the ANOVA for formability. In the experimental study, the percentage of the confidence level of feed rate is 29.04%, with a tool radius of 12.7% and a step depth of 53.25% on formability. In the numerical simulation study, the percentage of the confidence level of feed rate is 25.92%, with a tool radius of 22.56% and a step depth of 37.97% on formability. The values clearly show the step-depth is the main factor influencing the formability in both the numerical simulation (37.97% contribution) and the physical experiment (53.25% contribution).

Table 9: Analysis of variance for the maximum forming depth (Experimental)

Source	DF	SS	MS	F	P	P(%)
Feed Rate	2	1.77	0.88	5.85	0.14	29.04
Tool Radius	2	0.77	0.38	2.57	0.28	12.76
Step Depth	2	3.24	1.62	10.74	0.08	53.25
Error	2	0..30	0.15			
Total	8	6.09				

DF, degrees of freedom; F, variance; MS, mean square, P, test static, SS, sum of squares.

Table 10: Analysis of variance for the maximum forming depth (simulation)

Source	DF	SS	MS	F	P	P(%)
Feed Rate	2	2.13	1.07	1.91	0.34	25.92
Tool Radius	2	1.86	0.93	1.66	0.38	22.56
Step Depth	2	3.12	1.56	2.80	0.26	37.97
Error	2	1.12	0.56			
Total	8	8.227				

DF, degrees of freedom; F, variance; MS, mean square, P, test static, SS, sum of squares.

Interaction plot

The interaction plot for formability is shown in Figure 16 for the experimental study and numerical simulation respectively.

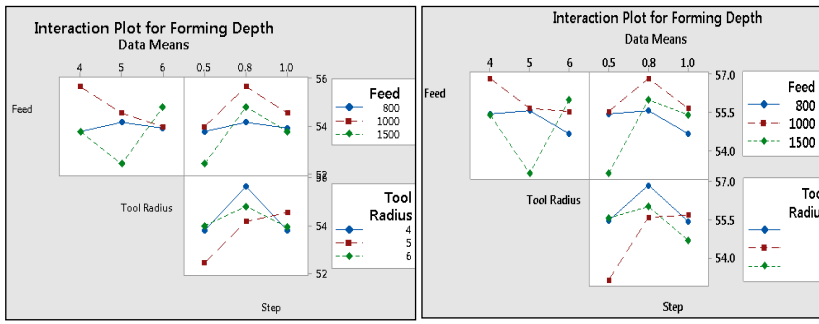

(a) (b)

Figure 16: Interaction plot (a) pysical experimental (b) numerical simulation

In both numerical simulation and experimental studies from the interaction of step depth with feed rate, the maximum formability was observed for the 0.8 step depth with a 1000 mm/min feed rate than other combinations. From the interaction of step depth with tool radius, the maximum formability was observed for the 0.8 step depth with a 4 mm tool radius than other combinations. From the interaction of feed rate with tool radius, the maximum formability was observed for the 1000 mm/min feed rate with a 4 mm tool radius than other tool radius and feed rate combination.

Conclusions

The present study appears to be the first study to investigate the effect of feed rate, forming tool radius, and step depth on the formability of drawing quality steel (CR2) based on IS 513: 2008 in SPIF. Using numerical simulation and physical experiment, the formability has been further optimized by a systematic experimental plan using Taguchi experiment design. From the results of the study, the following conclusion are made.

Bosetti and Bruschi [11] reported the fracture depth for a truncated cone with the wall angle formed using a 1.2 mm thick sheet of AA5182 aluminium alloy. The fracture depth was greater than 132 mm at the feed rate of 1000 mm/s and step depth of 0.8 mm and greater than 137 mm at a feed rate of 100 mm/s and step depth of 0.3 mm. Ziran et al. [36] evaluated the maximum wall angle for a U-shaped part using an AA-3003O aluminium sheet with a thickness of 1 mm. the maximum formability angle achieved using different tool diameter values was greater than 80°. Gulati et al. [34] conducted an optimization study using Taguchi design of experiment to found that optimum parameters for the maximum forming angle using

hyperbolic cone fabricated from an aluminium 6063 sheet the predicted optimal values for the wall angle found to be 88.29°. All the results reported by Bosetti and Bruschi [11], Ziran et al. [36], and Gulati et al. [34] shown that aluminium alloys are more formable than drawing quality steel in single point incremental forming.

- Results showed that the numerical simulation could predict the formability with a maximum error of below 6% when compared with the experimental values.
- The error between the experimental study and numerical simulation can be caused by fabrication error or mass scaling.
- The maximum formability is much associated with step depth. Its contribution is 53.25% in the experimental study and 55.4% in the numerical simulation.
- The average formability based on forming depth is 55.60 in the simulation and 54.12 in the fabrication and the error is 2.73%.
- The average formability based on the forming angle associate with this depth is 79.54 in the simulation and 76.43 in the fabrication and the error is 2.73%.

Reference

[1] R. Conte, G. Ambrogio, D. Pulice, F. Gagliardi and L. Filice, "Incremental Sheet Forming of a Composite Made of Thermoplastic Matrix and Glass-Fiber Reinforcement," *Procedia Engineering*, vol. 207, pp 819-824, 2017.

[2] M. A. Davarpanah, A. Mirkouei, X. Yu, R. Malhotra and S. Pilla, "Effects of incremental depth and tool rotation on failure modes and microstructural properties in Single Point Incremental Forming of polymers," *J. Mater. Process. Technol*., vol. 222, pp 287–300, 2015.

[3] C. Pandivelan and A. K. Jeevanantham, "Formability evaluation of AA 6061 alloy sheets on single point incremental forming using CNC vertical milling machine," *J. Mater. Environ. Sci.*, vol. 6, no. 5, pp 1343–1353, 2015.

[4] I. Bagudanch, M. L. Garcia-Romeu, G. Centeno, A. Elías-Zúñiga and J. Ciurana, "Forming force and temperature effects on single point incremental forming of polyvinylchloride," *J. Mater. Process. Technol.*, vol. 219, pp 221–229, 2015.

[5] X. Zhang, J. Wang and S. Zhang, "Study on Process Parameters on Single Point Incremental Forming of PVC," *Mater. Sci. Forum*, vol. 878, pp 74–80, 2017.

[6] X. Song, J. Zhang, W. Zhai, M. Taureza, S. Castagne and A. Danno, "Numerical and Experimental Study of Micro Single Point Incremental Forming Process," *Procedia Eng.*, vol. 207, pp 825–830, 2017.

[7] S. Kurra, N. Swetha, C. V. Reddy and S. P. Regalla, "Experimental and finite element studies of single stage incremental forming process : effect of process parameters on maximum wall angle and thickness distribution," *Adv. Mater. Process. Technol.*, vol. 0698, no. December, pp 1–13, 2017.

[8] V. Oleksik, A. Pascu and E. Avrigean, "Theoretical and Experimental Studies on the Influence of Process Parameters on Strains and Forces of Single Point Incremental Forming," *Adv. Mater. Res.*, vol. 939, pp 367–372, 2014.

[9] S. Golabi and H. Khazaali, "Determining frustum depth of 304 stainless steel plates with various diameters and thicknesses by incremental forming," *J. Mech. Sci. Technol.*, vol. 28, no. 8, pp 3273–3278, 2014.

[10] S. D. Majagi, G. Chandramohan and M. S. Kumar, "Effect Of Incremental Forming Process Parameters On Aluminum Alloy using Experimental Studies," *Adv. Mater. Res.*, vol. 1119, pp 633–639, 2015.

[11] Y. Li, Z. Liu, W. J. T, Bill. Daniel and P. A. Meehan, "Simulation and Experimental Observations of Effect of Different Contact Interfaces on the Incremental Sheet Forming Process," *Mater. Manuf. Process.*, vol. 29, no. 2, pp 121–128, 2014.

[12] V. Gulati, A. Aryal, P. Katyal and A. Goswami, "Process Parameters Optimization in Single Point Incremental Forming," *J. Inst. Eng. Ser. C*, vol. 97, no. 2, pp 185–193, 2015.

[13] D. S. Malwad and V. M. Nandedkar, "Deformation Mechanism Analysis of Single Point Incremental Sheet Metal Forming," *Procedia Mater. Sci.*, vol. 6, no. Icmpc, pp. 1505–1510, 2014.

[14] D. G. M. V. Naga chaitanya, Sunder singh sivam S.P and M. Gopal, "An Experimental Investigation on the Single Point Incremental Forming Of Aluminium," *Int. J. Eng. Res.*, vol. 3, no. Special 1, pp 155-159, 2014.

[15] E. H. Uheida, G. A. Oosthuizen and D. Dimitrov, "Investigating the Impact of Tool Velocity on the Process Conditions in Incremental Forming of Titanium Sheets," *Procedia Manuf.*, vol. 7, pp 345–350, 2017.

[16] Y. Zeradam and A. Krishnaiah, "Extraction of Coordinate Points for the Numerical Simulation of Single Point Incremental Forming Using Microsoft Excel," *International Conference on Emerging Trends in Engineering (ICETE): Learning and Analytics in Intelligent Systems*, vol. 2, pp 577-586, 2020.

[17] Y. Zeradam and A. Krishnaiah, "Numerical Simulation and Experimental Validation of Thickness Distribution in Single Point Incremental Forming for Drawing Quality Steel," *Int. J. Appl. Eng. Res.*, vol. 15, no. 1, pp 101–107, 2020.

[18] K Suresh, SD Bagade and SP Regalla, "Deformation behavior of extra deep drawing steel in single-point incremental forming," *Mater Manuf Process*, vol. 30, no. 10, pp 1202–1209, 2015.
[19] R. Ganesan, Research methodology for engineers. MJB Publishers, 2011.
[20] Y.Zeradam and A. Krishnaiah, "Spiral Toolpath Definition and G-code Generation for Single Point Incremental Forming," *J Mech Eng*, vol. 17, no. 1, pp 91-102, 2020.
[21] J. Jeswiet and D. Young, "Forming limit diagrams for single-point incremental forming of aluminium sheet," *Journal of Engineering Manufacture*, vol. 219, no. 4, pp 359–364, 2005.
[22] G Hussain, HR Khan, L Gao and N Hayat, "Guidelines for Tool-size Selection for Single-point Incremental Forming of an Aerospace Alloy," *Materials and Manufacturing Processes*, vol. 28, no. 3, pp 324–329, 2013.
[23] KA Ghamdi and G Hussain, "Threshold Tool-radius Condition Maximizing the Formability in SPIF Considering a Variety of Materials: Experimental and Fe Investigations," *International Journal of Machine Tools and Manufacture*, vol. 88, pp 82–94, 2014.
[24] T Obikawa, S Satou and T Hakutani, "Dieless Incremental Micro-forming of Miniature Shell Objects of Aluminum Foils," *International Journal of Machine Tools and Manufacture*, vol. 49, no.12–13, pp 906–915, 2009.
[25] G Hussain, L Gao, N Hayat and NU Dar ,"The Formability of Annealed and Pre-aged AA-2024 Sheets in Single-point Incremental Forming," *International Journal of Advanced Manufacturing Technology*, vol. 46, no. 5–8, pp 543–549, 2010.
[26] G Ambrogio and F Gagliardi, "Temperature Variation During High Speed Incremental Forming on Different Lightweight Alloys," *International Journal of Advanced Manufacturing Technology*, vol. 76, no.9–12, pp 1819–1825, 2015.